

A Gunn-Peterson test with a QSO at $z=6.4$

Tomotsugu Goto^{1,2} \star †, Yousuke Utsumi³, Takashi Hattori¹,
Satoshi Miyazaki³, and Chisato Yamauchi⁴

¹Subaru Telescope 650 North A'ohoku Place Hilo, HI 96720, USA

²Institute for Astronomy, University of Hawaii 2680 Woodlawn Drive, Honolulu, HI, 96822, USA

³Department of Astronomical Science, The Graduate University for Advanced Studies, 2-21-1 Osawa, Mitaka, Tokyo 181-8588, Japan

⁴Institute of Space and Astronautical Science, Japan Aerospace Exploration Agency, Sagami-hara, Kanagawa 252-5210

19 January 2013; in original form 2011 Feb 7

ABSTRACT

Understanding the cosmic re-ionization is one of the key goals of the modern observational cosmology. High redshift QSO spectra can be used as background light sources to measure absorption by intervening neutral hydrogen. We investigate neutral hydrogen absorption in a deep, moderate-resolution Keck/Deimos spectrum of QSO CFHQSJ2329-0301 at $z=6.4$. This QSO is one of the highest redshift QSOs presently known at $z=6.4$ but is 2.5 mag fainter than a previously well-studied QSO SDSSJ1148+5251 at $z=6.4$. Therefore, it has a smaller Stromgren sphere, and allows us to probe the highest redshift hydrogen absorption to date. The average transmitted flux at $5.915 < z_{abs} < 6.365$ (200 comoving Mpc) is consistent with zero, in Ly α , Ly β , and Ly γ absorption measurements. This corresponds to the lower limit of optical depth, $\tau_{eff}^{\alpha} > 4.9$. These results are consistent with strong evolution of the optical depth at $z > 5.7$.

Key words: quasars:individual, cosmology:early universe, black hole physics, galaxies: high-redshift

1 INTRODUCTION

Understanding when and how the neutral dark Universe was re-ionized by the first stars, galaxies, and black holes is a key goal of modern observational cosmology. The bright UV continuum of high-redshift QSOs can be used as a background light source to probe this cosmic re-ionization since it is absorbed by neutral hydrogen. Previously, Fan et al. (2006, F06 hereafter) compiled 19 QSOs at $5.74 \leq z < 6.42$ to find the sudden increase of optical depth (τ) and the length of dark gaps at $z \sim 6$, suggesting an approach to the end of the re-ionization.

However, increasing diversity has been observed in the optical depth in various line of sights, suggesting it is important to use a statistically significant sample size to discuss the evolution of optical depth. The highest redshift QSO previously used for absorption analysis, SDSSJ1148+5251 at $z=6.42$, had escaping flux detected at $z=6.25$ (Fan et al. 2003). This means there is still room for the QSO absorption measurement to be a useful probe of the cosmic re-ionization.

In this work, we observe QSO CFHQSJ2329-0301 at $z=6.4$ with the Keck/Deimos spectrograph. This QSO is ≈ 2.5 mag fainter than the previously well-studied highest redshift QSO SDSSJ1148+5251 at $z=6.4$. Therefore, the QSO has a few times

smaller Stromgren sphere (in radius), allowing us to measure optical depth much closer to the QSO emission at higher redshift. We measure the neutral hydrogen absorption in this QSO spectra to gain a better understanding of the evolution of the optical depth at high redshift.

Unless otherwise stated, we adopt the WMAP cosmology: $(h, \Omega_m, \Omega_L) = (0.7, 0.3, 0.7)$ (Komatsu et al. 2011).

2 OBSERVATION

Our target is a QSO CFHQSJ2329-0301 (Willott et al. 2007, W07 hereafter). Initially the redshift was reported to be $z=6.43$ based on Ly α (W07). The redshift was later corrected to be $z=6.417$ based on the Mg II line (Willott et al. 2010) because blueward of the Ly α emission line suffers from heavy absorption from neutral hydrogen. This is one of the three highest redshift QSOs to date, along with SDSSJ1148+5251 at $z=6.419$ (Fan et al. 2003) and CFHQS0210-0456 at $z=6.438$ (Willott et al. 2010). This QSO is known to be in a dense environment surrounded by 7 Lyman break galaxies (LBGs) (Utsumi et al. 2010) and to have extended Ly α emission and continuum (Goto et al. 2009). Characteristics of the target are summarized in Table 1.

We obtained moderate resolution spectra of the QSO using Keck/Deimos (Faber et al. 2003) on Sep. 12-13, 2010. Although Deimos was used in the multi-slit mode to investigate the environment of the QSO, we focus on the QSO spectra in this paper. We

\star E-mail: tomo@ifa.hawaii.edu

† JSPS SPD Fellow

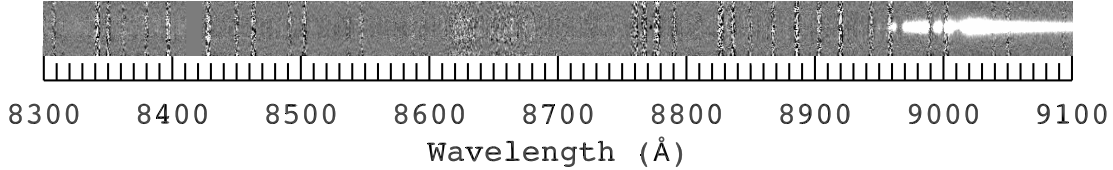


Figure 1. Two dimensional spectra of CFHQSJ2329-0301, taken with the Keck/Deimos spectrograph. One-dimensional spectrum is shown in Fig. 2.

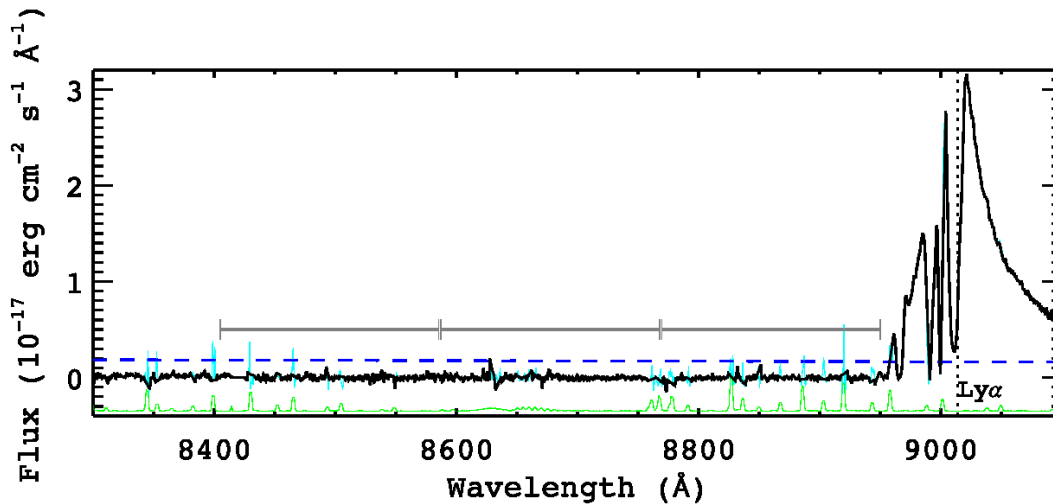


Figure 2. One-dimensional spectra of CFHQSJ2329-0301. The blue dashed line shows the best-fit continuum level, assuming a power law of $f_\nu \propto \nu^{-0.5}$. The cyan lines show the wavelengths masked out due to the strong sky emissions. The green lines show the sky spectrum in arbitrary units. The gray lines show the first three wavelength regions where the flux was consistent with zero. The corresponding two-dimensional spectrum is shown in Fig. 1.

used the 830 lines mm^{-1} grating and the OG550 filter with a central wavelength of 8000\AA . This setting has a wavelength coverage of 6000\AA to 10000\AA with a spectral resolution of $\sim 2.5\text{\AA}$ for $0.75''$ slit. The spatial resolution is $0.1185'' \text{ pixel}^{-1}$. The total integration time was 5.5 hours.

We used the DEEP2 pipeline (Wirth et al. 2004; Davis et al. 2007) to reduce the data, except the background subtraction, which we did manually to remove ghost features of the 830 grating. Wavelength calibration is based on the HeNeAr lamp. The spectrophotometric standard G191-B2B was observed and used for flux calibration. Fig. 1 shows two-dimensional spectrum of the QSO.

At $>7500\text{\AA}$, many strong sky OH emission lines are present. Although the DEEP2 pipeline subtracts these sky lines well, the noise level at the exact wavelengths of the sky lines are significantly higher than the other wavelength clear of emission. Therefore, we have masked out these wavelengths of strong sky emissions from the absorption measurement. In Fig. 2, the wavelengths masked out are shown in thin cyan lines. The green lines at the bottom show the sky spectrum in arbitrary units. We checked that this procedure only affects our measurements at the few per cent level, and does not change the main conclusion of the paper.

We used double Gaussians to fit $\text{Ly } \alpha$ and NV lines. The double-gaussian model do not fit the observed spectra well due to the heavy absorption blueward of $\text{Ly } \alpha$ and broad natures of both lines. The best-fit rest-frame equivalent widths are $110 \pm 60\text{\AA}$, and

$6 \pm 1\text{\AA}$ for $\text{Ly } \alpha$ and NV, respectively. These values are consistent with previously reported values (W07).

The spectrum shows four strong $\text{Ly } \alpha$ absorptions on the blue-side of the emission (Fig. 2). There also exist absorption lines at 9183 , 9212 , and 9240\AA with equivalent widths of 1.4 , 1.5 and 2.6\AA , respectively. Because none of the pairs corresponds to different lines of the same system (such as $\text{SiII}\lambda 1260$, $\text{SiII}\lambda 1304$, $\text{OI}\lambda 1302$, and $\text{CII}\lambda 1334$), the identities of these lines are not clear. There also is an emission line at 9681\AA , corresponding to OI line (1302.17\AA) at $z=6.43$.

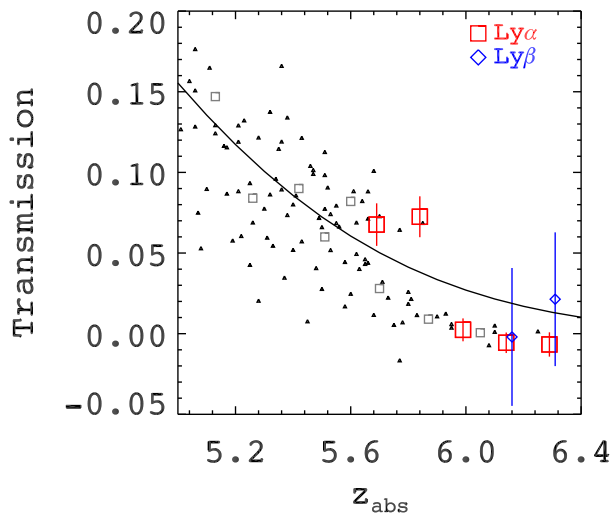
3 ABSORPTION MEASUREMENTS AND RESULTS

High redshift QSOs can be used as a background light source to investigate the inter-galactic medium (IGM) at high redshift. In the following subsections, we measure average absorption in the $\text{Ly } \alpha$, $\text{Ly } \beta$, and $\text{Ly } \gamma$ forest regions.

To measure the IGM absorption, we need to determine the continuum before the absorption. This is not a trivial process because the continuum blueward of the $\text{Ly } \alpha$ is heavily absorbed by the neutral hydrogen. At the same time, our optical CCD loses sensitivity at around $10,000\text{\AA}$, and we do not have a long baseline to fit continuum, let alone the presence of strong $\text{Ly } \alpha$, NV and OI emissions. Following previous work by Fan et al. (2000, 2001), we as-

Table 1. Target information adopted from Willott et al. (2007) and Goto et al. (2009).

Object	z_{MgII}	i'_{AB}	z'_{AB}	z_R	J
CFHQS J232908.28-030158.8	6.417 ± 0.002	25.54 ± 0.02	21.165 ± 0.003	21.683 ± 0.007	21.56 ± 0.25

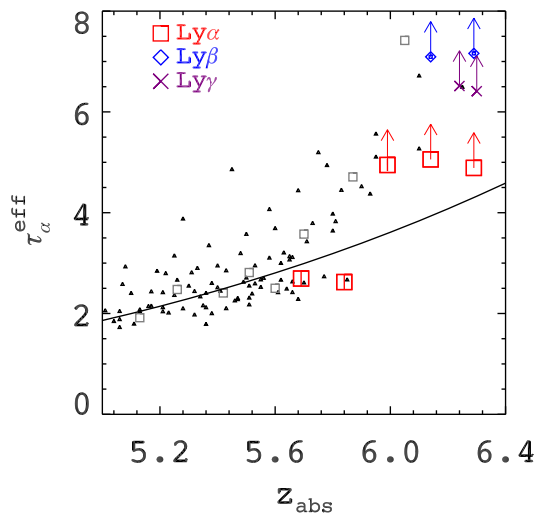

Figure 3. Lyman transmission in the spectrum of CFHQSJ2329-0301 (red, filled-circles). The black triangles are from Fan et al. (2006), and the gray squares are from Songaila (2004).

sume a power-law continuum of $f_\nu \propto \nu^{-0.5}$. When the continuum slope is uncertain, the slope of $\nu^{-0.5}$ is commonly used by previous works. This is the case for most QSOs at $z \sim 6$. We fit the continuum of $\nu^{-0.5}$ to the spectrum at $> 9300 \text{\AA}$ to determine the continuum level. We also follow Fan et al. (2000, 2001) to consider variation from $\nu^{+0.5}$ to $\nu^{-1.5}$ to estimate errors of τ . However, this is a conservative approach since at least at lower z , most QSO continuum slopes are between -0.3 and -0.9 (e.g., Vanden Berk et al. 2001). Some recent papers do not even include variation of the slope in the errors of τ . In this work, errors in the continuum fit and the variation in the slope are included in the final uncertainty in the transmission. Based on this continuum, we measure average transmission in the following narrow wavelength (redshift) windows. Then, the transmission is used to calculate the effective optical depth.

3.1 Ly α absorption

With QSO CFHQSJ2329-0301, we can measure absorption closer to the Ly α emission than bright QSOs, because this QSO has a small Stromgren sphere (ionized zone) of 6.4 Mpc (where Ly α flux drops first to $T < 0.1$ for spectra binned in $20 \text{\AA} \text{ pixel}^{-1}$) due to its faint intrinsic luminosity (W07). To measure absorption, we used the maximum redshift, z_{max} , of 6.365, where blue-ward of continuum does not show any sign of rise. This gives us $z_{\text{em}} - z_{\text{max}} = 0.052$. This is the highest redshift absorption measurement from the QSO spectra to date due to the high redshift of QSO ($z=6.4$) and its small Stromgren sphere.

We measure Ly α absorption down to 1040\AA , which is the shortest wavelength that is not affected by the Ly β +OVI emissions.


Figure 4. Effective Gunn-Peterson optical depth from the spectrum of CFHQSJ2329-0301 (red, filled-circles). The black triangles are from Fan et al. (2006), and the gray squares are from Songaila (2004). The solid line is the best power-law fit to the data at $z < 5.5$ by F06 (eq.5).

Within this range, we used the redshift interval of Δz of 0.15, which corresponds to ~ 60 Mpc in comoving distance, for comparison with previous work. Although the resolution of our spectrum is lower than high-resolution spectra used in the past, this is not a disadvantage for a binned measurement like the transmission. The first three bins are shown in gray horizontal lines in Fig. 2. The median redshifts of five bins are presented in Table 2. Using this redshift range and interval, we measure the transmission as

$$\mathcal{T}(z_{\text{abs}}) \equiv \langle f_\nu^{\text{obs}} / f_\nu^{\text{int}} \rangle$$

The measured transmitted flux (\mathcal{T}) is shown in Table 2 and plotted in Fig. 3. We estimate errors by changing the continuum slope from $\nu^{+0.5}$ to $\nu^{-1.5}$, quadruply added by the noise in spectra and the errors in determining the continuum level. The errors on \mathcal{T} are dominated by the continuum determination.

In Fig. 3 and Table 2, the first three bins at $5.915 < z < 6.365$ have no detected flux and are consistent with zero within the error. Only two lower redshift bins at $5.615 < z < 5.915$ have detected flux.

It is conventional to express optical depth τ in terms of $\tau = -\ln(\mathcal{T})$. We present τ as a function of redshift in Fig. 4. For bins where we do not have detected flux, we convert the errors on \mathcal{T} to the lower limit of the τ .

In Figs.3 and 4, small triangles and gray squares represent previous data from F06 and Songaila (2004). The solid line shows the best power-law fit to the data at $z < 5.5$ by F06 (eq.5).

Table 2. IGM absorption towards the QSO CFHQSJ2309-0301 at $z = 6.42$. The widths of bins are $\Delta z = 0.15, 0.15$, and 0.06 for $\text{Ly } \alpha$, $\text{Ly } \beta$, and $\text{Ly } \gamma$ absorptions, respectively.

Redshift	Line	Transmission	τ_α
6.29	$\text{Ly } \alpha$	-0.007 ± 0.008	> 4.9
6.14	$\text{Ly } \alpha$	-0.006 ± 0.006	> 5.1
5.99	$\text{Ly } \alpha$	0.002 ± 0.007	> 4.9
5.84	$\text{Ly } \alpha$	0.073 ± 0.013	2.6 ± 0.1
5.69	$\text{Ly } \alpha$	0.068 ± 0.013	2.7 ± 0.2
6.29	$\text{Ly } \beta$	0.021 ± 0.041	> 7.2
6.14	$\text{Ly } \beta$	-0.002 ± 0.043	> 7.1
6.29	$\text{Ly } \gamma$	0.26 ± 0.23	> 6.4
6.23	$\text{Ly } \gamma$	-0.08 ± 0.23	> 6.5

3.2 $\text{Ly } \beta$ absorption

At the same neutral hydrogen density, the optical depth τ is proportional to $f\lambda$, where f and λ are the oscillator strength and rest-frame wavelength of the transition. Therefore, the τ of $\text{Ly } \beta$ is factor of 6.2 smaller than that of $\text{Ly } \alpha$. Thus, $\text{Ly } \beta$ can probe into much more neutral hydrogen than $\text{Ly } \alpha$ absorption. In this section we measure optical depth using $\text{Ly } \beta$ absorption from the spectra.

We assume the same continuum as was used for $\text{Ly } \alpha$. We choose the minimum redshift of $\text{Ly } \beta$ as 970\AA , above which it is not affected by $\text{Ly } \gamma$ absorption. This leaves us the redshift range of $6.065 < z_{\text{abs}} < 6.365$. The $\text{Ly } \beta$ absorptions overlap with $\text{Ly } \alpha$ absorption from lower redshift. Therefore, the $\text{Ly } \alpha$ absorption has to be corrected in measuring τ^β . We used eq. (5) of F06 to estimate $\text{Ly } \alpha$ absorption from lower redshift, and corrected the $\text{Ly } \beta$ transmission measurements.

Table. 2 shows the results. They are also plotted in Fig. 3 with the blue diamonds. No flux is detected in $\text{Ly } \beta$ measurements. The two measured $\text{Ly } \beta$ transmissions at $6.065 < z_{\text{abs}} < 6.365$ are consistent with zero flux within the error.

To convert $\text{Ly } \beta$ transmission to τ_β , one has to consider different optical depths between $\text{Ly } \alpha$ and $\text{Ly } \beta$. The difference depends on the UV background, clumpiness of the IGM, its equation of state, and the uniformity of the UV background. According to simulations (e.g., Oh & Furlanetto 2005) and empirical measurements (F06), the τ_α/τ_β conversion is in the range of 2.5-2.9. The τ_α/τ_γ conversion lies in the range of 4.4-5.7. Following the discussion in F06, we use $\tau_\alpha/\tau_\beta=2.25$ and $\tau_\alpha/\tau_\gamma=4.4$.

Fig. 4 shows constraints on the τ_α from $\text{Ly } \beta$ absorption measurements. Note that τ is converted to $\text{Ly } \alpha$ optical depth in Fig. 4. Since flux are not detected in both bins, Table 2 shows the lower limit in τ_α from the error.

3.3 $\text{Ly } \gamma$ absorption

Similarly to $\text{Ly } \beta$, the $\text{Ly } \gamma$ optical depth is a factor of 17.9 smaller than that of $\text{Ly } \alpha$, providing us with a chance to probe into more neutral hydrogen. However, the $\text{Ly } \gamma$ absorption measurement is restricted by the presence of $\text{Ly } \delta$ absorption at the low-redshift end and the QSO flux at the high-redshift end. Therefore, we use a smaller bin size of Δz of 0.06. The $\text{Ly } \gamma$ transmission measurements are corrected for overlapping lower redshift $\text{Ly } \alpha$ and $\text{Ly } \beta$ absorptions using the best-fit power laws to lower redshift data (eqs. 5 and 6 in F06). The optical depth is converted to the τ_α , using $\tau_\alpha/\tau_\gamma=4.4$. The results are in Table 2 and Fig. 4.

The $\text{Ly } \gamma$ transmission has more potential since it has a factor of 17.9 smaller optical depth. However, the $\text{Ly } \gamma$ absorption measurements are much more challenging. Since the overlapping foreground $\text{Ly } \alpha$ and $\text{Ly } \beta$ lines absorb $\sim 98\%$ of the continuum flux in the wavelength ranges of $\text{Ly } \gamma$, so we need to measure absorption in the remaining $\sim 2\%$. Errors in continuum determination are also larger since we use the bluer part of the spectrum. By just changing the slope of $\nu^{+0.5}$ to $\nu^{-1.5}$, we get 10% error in the measurement. Combined with the noise in the spectra, we did not obtain tighter constraints than $\text{Ly } \beta$. The purple crosses in Fig. 4 show the lower limit from the measurement error.

4 DISCUSSION

It has often been suggested that QSOs are an ineffective re-ionization probe because $\text{Ly } \alpha$ absorption saturate at neutral hydrogen fractions of $f_{\text{HI}} \sim 10^{-4}$. However the Gunn-Peterson optical depths of $\text{Ly } \beta$ and $\text{Ly } \gamma$ are factors of 6.2 and 17.9 smaller than that of $\text{Ly } \alpha$. It has also been suggested that metal lines such as OI can be used to probe into even larger optical depths (Becker et al. 2006, 2011). While the dark gap statistic method can also probe into more neutral hydrogen (Songaila & Cowie 2002; Pentericci et al. 2002), our medium resolution spectrum did not allow us to measure the dark gaps. Although we did not detect any flux at $5.915 < z_{\text{abs}} < 6.365$, another $z=6.4$ QSO had a flux detected at $z=6.29$ with $\text{Ly } \gamma$ (F06). Therefore, there is room for high- z QSOs to be an important re-ionization probe beyond $z=6.4$. Also in both Figs. 3 and 4, τ and \mathcal{T} show a significant variation, which suggests the importance of finding more bright QSOs at $z > 6.4$ as an end of re-ionization probe. On-going and future imaging surveys at $> 1\mu\text{m}$ such as UKIDSS, VISTA, CFHQSIR, and PanSTARRS are expected to find such QSOs in the near future.

One of the remaining problems is an uncertainty in continuum determination. We used a slope of $\nu^{-0.5}$, but $\nu^{+0.5}$ and $\nu^{-1.5}$ also fit continuum at $> 9300\text{\AA}$ well. Variation from these is larger than the errors on the flux, even with our relatively short exposure of a faint QSO. Ironically, it is hard to measure intrinsic continuum blueward of $\text{Ly } \alpha$ emission because of the heavy absorption that we aim to measure. To make the matter worse, observations of a larger sample of QSOs at lower redshift show a continuum break at $1200 < \lambda < 1300\text{\AA}$, with a steeper power-laws of $\nu^{-1.7}$ at shorter wavelengths (Telfer et al. 2002). If there is an evolution, the continuum blueward of high- z QSOs remain uncertain. Therefore, the continuum determination is a problem in measuring τ even if one takes very high S/N spectra.

Interpretation of the evolution of τ is a matter of active debate. At $z > 5.7$, F06 reported a departure of τ from the best-fit power law from $z < 5.5$, arguing that $z \sim 6$ is the end of the reionization, where the Universe was not completely ionized. The average length of dark absorption gap also jumps from < 10 to > 80 comoving Mpc at $z > 5.7$. Our τ measurements are clearly above the solid line (fit to the $z < 5.5$ data) in Fig. 4, and thus are consistent with this sudden increase of τ at $z > 5.7$. On the other hand, Becker, Rauch, & Sargent (2007) showed that the probability distribution of $\text{Ly } \alpha$ transmitted flux of QSOs at $2 < z < 5$ are better fit by lognormal optical depth distributions. This lognormal fit is consistent with $z > 5.8$ data for no evolution in the hydrogen neutral fraction. However, W07 pointed out that the lognormal fit does not reproduce the data at $5.4 < z < 5.7$.

In either case, the large variation in the τ is the primary reason why determining a more realistic model is difficult. Although our

results add τ measurements at the highest redshift probed by QSO absorption, it is clear that we need a statistically significant sample (>20) of bright QSOs in every $\Delta z=0.1$ at $z > 6$, where τ quickly increases, to overcome cosmic variation of τ and more accurately trace the evolution of τ .

5 SUMMARY

Using a deep, medium-resolution Keck/Deimos spectra of a QSO at $z=6.4$, we measured neutral hydrogen absorption, and thereby, the optical depth. Because our QSO is by 2.5 mag fainter than the previously studied QSO SDSSJ1148+5251 at $z=6.4$, we can investigate absorption much closer to the QSO emission, reaching $z=6.365$, the highest absorption redshift investigated to date. Our measurement of transmitted flux is consistent with zero at $5.915 < z_{abs}^{\alpha} < 6.365$ in all $\text{Ly}\alpha$, $\text{Ly}\beta$, and $\text{Ly}\gamma$ measurements. We obtained a lower limit of $\tau^{\alpha} > 4.8$. These results are consistent with strong evolution of the optical depth at $z > 5.7$.

ACKNOWLEDGMENTS

We thank the anonymous referee for many insightful comments, which significantly improved the paper. We are grateful to Michael Koss for useful discussion, Hisanori Furusawa and Yutaka Komiyama for providing their Subaru/Suprimecam data of the target. We thank M. Cooper, J. Newman, and B. Lemaux for their assistance in using the DEEP2 pipeline.

T.G. acknowledges financial support from the Japan Society for the Promotion of Science (JSPS) through JSPS Research Fellowships for Young Scientists.

This work is supported in part with the research fund for students (2010) of the Department of Astronomical Science, the Graduate University for Advanced Studies, Japan.

The authors wish to recognize and acknowledge the very significant cultural role and reverence that the summit of Mauna Kea has always had within the indigenous Hawaiian community. We are most fortunate to have the opportunity to conduct observations from this sacred mountain.

REFERENCES

- Becker G. D., Rauch M., Sargent W. L. W., 2007, ApJ, 662, 72
- Becker G. D., Sargent W. L. W., Rauch M., Simcoe R. A., 2006, ApJ, 640, 69
- Becker G. D., et al., arXiv:1101.4399
- Davis M., et al., 2007, ApJ, 660, L1
- Faber S. M., et al., 2003, SPIE, 4841, 1657
- Fan X., et al., 2006, AJ, 132, 117
- Fan X., et al., 2003, AJ, 125, 1649
- Fan X., et al., 2001, AJ, 122, 2833
- Fan X., et al., 2000, AJ, 119, 928
- Goto T., Utsumi Y., Furusawa H., Miyazaki S., Komiyama Y., 2009, MNRAS, 400, 843
- Komatsu E., et al., 2011, ApJS, 192, 18
- Oh S. P., Furlanetto S. R., 2005, ApJ, 620, L9
- Oke J. B., Korycansky D. G., 1982, ApJ, 255, 11
- Pentericci L., et al., 2002, AJ, 123, 2151
- Songaila A., 2004, AJ, 127, 2598
- Songaila A., Cowie L. L., 2002, AJ, 123, 2183

- Telfer R. C., Zheng W., Kriss G. A., Davidsen A. F., 2002, ApJ, 565, 773
- Utsumi Y., Goto T., Kashikawa N., Miyazaki S., Komiyama Y., Furusawa H., Overzier R., 2010, ApJ, 721, 1680
- Vanden Berk D. E., et al., 2001, AJ, 122, 549
- Willott C. J., et al., 2010, AJ, 140, 546
- Willott C. J., et al., 2007, AJ, 134, 2435
- Wirth G. D., et al., 2004, AJ, 127, 3121